

Accelerating rate calorimetry studies of the reactions between ionic liquids and charged lithium ion battery electrode materials

Yadong Wang^a, K. Zaghbi^b, A. Guerfi^b, Fernanda F.C. Bazito^{c,1},
Roberto M. Torresi^c, J.R. Dahn^{a,*}

^a Department of Physics and Atmospheric Science, Dalhousie University, Halifax, NS, Canada B3H 3J5

^b Institut de Recherche d'Hydro-Quebec, 1800 Lionel-Boulet, Varennes, Que., Canada J3X 1S1

^c Instituto de Química Universidade de São Paulo, CP 26077, 05513-970 São Paulo, Brazil

Received 7 February 2007; received in revised form 4 April 2007; accepted 8 April 2007

Available online 25 April 2007

Abstract

Using accelerating rate calorimetry (ARC), the reactivity between six ionic liquids (with and without added LiPF_6) and charged electrode materials is compared to the reactivity of standard carbonate-based solvents and electrolytes with the same electrode materials. The charged electrode materials used were Li_1Si , $\text{Li}_7\text{Ti}_4\text{O}_{12}$ and $\text{Li}_{0.45}\text{CoO}_2$. The experiments showed that not all ionic liquids are safer than conventional electrolytes/solvents. Of the six ionic liquids tested, 1-ethyl-3-methylimidazolium bis(fluorosulfonyl)imide (EMI-FSI) shows the worst safety properties, and is much worse than conventional electrolyte. 1-Ethyl-3-methylimidazolium bis(trifluoromethanesulfonyl)imide (EMI-TFSI) and 1-propyl-1-methylpyrrolidinium bis(fluorosulfonyl)imide (Py13-FSI) show similar reactivity to carbonate-based electrolyte. The three ionic liquids 1-butyl-2,3-dimethylimidazolium bis(trifluoromethanesulfonyl)imide (BMMI-TFSI), 1-butyl-1-methylpiperidinium bis(trifluoromethanesulfonyl)imide (Pp14-TFSI) and *N*-trimethyl-*N*-butylammonium bis(trifluoromethanesulfonyl)imide (TMBA-TFSI) show similar reactivity and are much safer than the conventional carbonate-based electrolyte. A comparison of the reactivity of ionic liquids with common anions and cations shows that ionic liquids with TFSI^- are safer than those with FSI^- , and liquids with EMI^+ are worse than those with BMMI^+ , Py13^+ , Pp14^+ and TMBA^+ .

© 2007 Elsevier Ltd. All rights reserved.

Keywords: Lithium-ion batteries; Ionic liquids; Safety; Accelerating rate calorimetry

1. Introduction

The large reaction heat between charged electrode materials and the non-aqueous electrolyte ultimately is the cause of safety issues involving lithium-ion batteries in the field. To improve the safety of Li-ion batteries, this reaction heat should be reduced, and/or the kinetics of the reactions slowed. A number of successful approaches have been identified, involving electrode materials of minimum specific surface area [1], alternative electrode material chemistries that show improved safety [2] and new electrolyte solvents and salts [3].

During the past decade, ionic liquids have been proposed as alternative electrolyte solvents for Li-ion batteries [4–14] because of their claimed advantages of non-flammability, no detectable vapor pressure up to 200 °C, high chemical and thermal stability, high ionic conductivity, low toxicity, and, in some cases, hydrophobicity as compared to conventional flammable aprotic organic solvents [15,16]. However, lithium secondary batteries using ionic liquids as electrolyte solvents generally showed poor properties compared to those with conventional alkylcarbonate-based electrolyte. Besides the disadvantages of high viscosity and high cost, most ionic liquids do not form a robust solid electrolyte interphase on the surface of the carbon negative electrode during the first lithiation. Therefore, most of the research activity in the area of ionic liquids for Li-ion batteries has focused on identifying new ionic liquids and new additives in order to improve charge–discharge cycling performance.

* Corresponding author.

E-mail address: jeff.dahn@dal.ca (J.R. Dahn).

¹ Present address: Universidade Federal de São Paulo, Campus de Diadema, Diadema (SP), Brazil.

There is very little direct experimental evidence to suggest that Li-ion cells using ionic liquids as electrolyte solvents are really safer than those that use conventional organic electrolytes. Only recently, Egashira et al. [17], using differential scanning calorimetry (DSC), showed that an electrolyte made of a mixture of two ionic liquids (cyanomethyl trimethyl ammonium bis(trifluoromethane)sulfoneimide and 1-ethyl-3-methyl imidazolium bis(trifluoroethane)sulfoneimide) exhibited an exothermic reaction with $\text{Li}_{0.46}\text{CoO}_2$ that began at around 260°C , which is about 90°C higher than conventional carbonate-based electrolytes. Sakaebe et al.'s DSC experiment indicates that Pp13-TFSI shows a much lower onset temperature compared with organic carbonate-based electrolytes when $\text{Li}_{1-x}\text{Ni}_{1/3}\text{Mn}_{1/3}\text{Co}_{1/3}\text{O}_2$, $\text{Li}_{1-x}\text{CoO}_2$ or lithium metal was used [14]. These results suggest that the use of ionic liquids can lead to safer Li-ion cells. Nevertheless, it cannot be concluded from these experiments that all the ionic liquids are better from a safety standpoint than carbonate-based electrolytes. Furthermore, the reactivity of the ionic liquids with both the charged positive electrode and the charged negative electrode must be considered.

In this paper, the reactivity of six ionic liquids incorporating common cations and anions with charged positive and negative electrode materials is studied using accelerating rate calorimetry (ARC) methods.

2. Experimental

2.1. Ionic liquid preparation

Fig. 1 shows the chemical structures of the six ionic liquids investigated in this work. The ionic liquids 1-methyl-3-ethyl

imidazolium bis-trifluoromethanesulfonimide (EMI-TFSI) and 1-methyl-3-ethyl imidazolium bis-fluorosulfonimide (EMI-FSI) were prepared in the Hydro-Quebec (IREQ) laboratory using a variation of the HQ patented synthesis [18–20]. Fifteen grams of 1-methyl-3-ethyl imidazolium chloride (EMICl) was dissolved in 100 ml of water to which 23 g of potassium bis-trifluoromethanesulfonimide (KTFSI) had been previously added. A separation into two liquid phases occurred. The EMI-TFSI molten salt was extracted with dichloromethane and dried with anhydrous magnesium sulfate. The suspension was filtered and the solvent was evaporated. The salt was dried under vacuum at 90°C . In the case of EMI-FSI ionic liquid, the preparation method was the same as for EMI-TFSI except that KTFSI was replaced by KFSI. Their purity was checked using slow cyclic voltammetry. Water content was measured by a Karl Fisher titration and was less than 15 ppm.

The ionic liquids *N*-methyl-*N*-propylpyrrolidinium-FSI (Py13-FSI), *N*-trimethyl-*N*-butylammonium-TFSI (TMBA-TFSI) and 1-butyl-1-methylpiperidinium-TFSI (Pp14-TFSI) were purchased from Dai-ichi Kogyo Seuyaku Co. Ltd. (Kyoto, Japan).

In order to remove H_2O from the ionic liquids, a new purification method developed by Hydro-Quebec [20] was used. In this method the ionic liquid was reacted with CaC_2 in an argon glove box, forming $\text{Ca}(\text{OH})_2$ and acetylene. After centrifugation and phase separation, the water content was less than 15 ppm. The LiTFSI salt was obtained from 3M Company (USA) and the LiFSI salt was obtained from University of Montreal (Québec, Canada). These salts were used in the conductivity measurements at a concentration of 0.5 M.

The conductivity measurements were performed using a model CM-30R conductivity meter (from DKK-TOA Corp.,

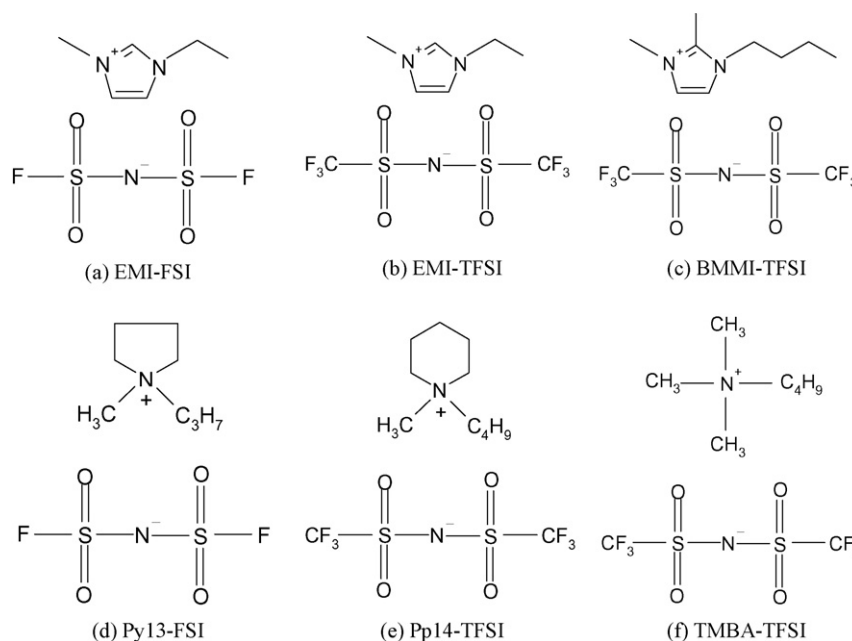


Fig. 1. Chemical structures of (a) 1-ethyl-3-methylimidazolium bis(fluorosulfonyl)imide (EMI-FSI), (b) 1-ethyl-3-methylimidazolium bis(trifluoromethanesulfonyl)imide (EMI-TFSI), (c) 1-butyl-2,3-dimethylimidazolium bis(trifluoromethanesulfonyl)imide (BMMI-TFSI), (d) 1-propyl-1-methylpyrrolidinium bis(fluorosulfonyl)imide (Py13-FSI), (e) 1-butyl-1-methylpiperidinium bis(trifluoromethanesulfonyl)imide (Pp14-TFSI), and (f) *N*-trimethyl-*N*-butylammonium bis(trifluoromethanesulfonyl)imide (TMBA-TFSI).

Table 1
The viscosity and conductivity of the six ionic liquids and EC:DEC with or without salt^a

Ionic liquid	Viscosity at (cP)	Conductivity (mS/cm)			
		No salt added	+0.5 M LiTFSI	+0.5 M LiFSI	+1 M LiPF ₆
EMI-FSI	19	17.74	12.38		
Py13-FSI	39	9.14	5.75	6.06	
EMI-TFSI	35	8.99	6.52		
Pp13-TFSI	151	1.47	0.98		
TMBA-TFSI	145	1.90	1.273		
BMMI-TFSI	5.3	1.97			
EC	1.93 ^b [21]	1 × 10 ⁻⁷ to 3 × 10 ^{-7b} [22]			
DEC	0.75 ^c [21]				
EC:DEC (1:2 vol)					7.24 ^c [23]

^a The temperature is 20 °C unless stated otherwise.

^b At 40 °C.

^c At 25 °C.

Japan). The viscosity was determined in the temperature range of –20 to 80 °C using an MCR-30 viscometer (Anton-Paar, USA). The viscosity values were measured at 20 °C. Table 1 shows the conductivity and viscosity measurements for five of the ionic liquids.

1-Butyl-2,3-dimethylimidazolium bis(trifluoromethanesulfonyl)imide (BMMI-TFSI) was synthesised at the Instituto de Química Universidade de São Paulo. In a flask fitted with a reflux condenser were added 1 mmol of 1,2 dimethylimidazole and 1 mmol of *n*-butyl bromide. After addition, the mixture was stirred at 140 °C for 1 h to give a white solid. This solid was recrystallized from acetonitrile and THF and dried under reduced pressure to give BMMIBr as white crystals. In another flask, 1 mmol of BMMIBr was placed and dissolved in 5.0 ml of water followed by an aqueous solution of 1.05 mmol LiTFSI in 5.0 ml of water. The reaction mixture was stirred overnight at room temperature and two phases were formed and separated. The phase containing the ionic liquid was washed several times with water, treated with activated carbon and subjected to column chromatography (alumina, dichloromethane). The ionic liquid was dried under reduced pressure for 3 days at 100 °C to give BMMI-TFSI as a colorless liquid. The BMMI-TFSI NMR data have been previously published [24].

2.2. Preparation of lithiated negative and delithiated positive electrode materials

Commercially available silicon (–325 mesh, Aldrich) was used as a starting material for the electrochemical formation of lithium silicon alloys. The BET (Brunauer–Emmett–Teller) specific surface area of the silicon powder was 1.04 m²/g. The silicon powder (80% by mass), super-S carbon (12%), polyvinylidene difluoride (PVDF, 8%) and *n*-methyl pyrrolidone (NMP, twice by mass of Si) were mixed into a slurry by gentle mechanical milling. After drying, the electrode powder was ground in a mortar and pestle and passed through a 300 μm screen. About 80 ± 1 mg of electrode powder was put into a die along with a circular piece of stainless steel mesh to act as a

support for the thin pellet. The pellet was pressed with 1000 bar pressure.

Li/Si coin cells with silicon pellet electrodes were discharged using capacity control to form nominal Li₁Si, (including irreversible capacity) using a current density of ca. 6.5 mA/g. After the discharge was completed, the coin cells were opened in an argon-filled glove box and disassembled. The Li₁Si electrode powder was rinsed with dimethyl carbonate (DMC) four times and dried under vacuum to remove the electrolyte [25]. The electrochemical synthesis procedure for the lithium silicon alloy, Li₁Si, is the same as that used in Ref. [26].

Li₇Ti₅O₁₂ was obtained by lithiating Li₄Ti₅O₁₂ (NEI Corporation, USA). The BET specific surface area of Li₄Ti₅O₁₂ was 4 m²/g. Li₄Ti₅O₁₂ pellet-type electrodes were made using the same procedure as for the silicon, except that the pellets were about 300 mg in mass and did not require a stainless steel mesh for support. Cells assembled with Li₄Ti₅O₁₂ pellet positive electrodes and lithium metal negative electrodes were discharged to 1.3 V versus lithium at a rate of C/50. After reaching 1.3 V, the cells relaxed for 30 min, and then the cells were discharged again to 1.3 V. After four such iterations, where the current was halved after each relaxation period, the cells were opened and rinsed in the same way as for the Li₁Si.

Battery grade LiCoO₂ was obtained from E-One Moli Energy Ltd. The BET specific surface area of the LiCoO₂ was 0.18 m²/g. LiCoO₂/lithium pellet cells were made in the same way as for silicon. The pellet cells were charged to 4.2 V versus lithium using a current of 3.5 mA/g. After reaching 4.2 V, the cells were allowed to relax for 30 min, and then were charged to 4.2 V again at the half of first charge current. This process was repeated four times, and a specific capacity of 150 mAh/g was obtained. Then the cells were opened and the electrode powder was rinsed in the glovebox in the same way as for Li₁Si. According to the specific capacity, the composition of the delithiated LiCoO₂ should be Li_{0.45}CoO₂.

The charged electrode powders were never exposed to air and 1 M LiPF₆ EC:DEC was used for all these coin cells that were prepared in order to charge or discharge the electrode materials.

2.3. ARC sample preparation

The ARC sample holder was made from 304 stainless steel seamless tubing with a wall thickness of 150 μm . The outer diameter of the tubing is 6 mm and the length of pieces cut for the ARC sample holders is 38 mm. One end of the tubing is flattened and welded shut using a tungsten inert gas (TIG) welder. After a known mass of electrode powder (when the mass of Li_1Si , $\text{Li}_7\text{Ti}_5\text{O}_{12}$ or $\text{Li}_{0.45}\text{CoO}_2$ is indicated, it also includes the mass of binder and conductive carbon black) and solvent were added to the tubing, the other end of the tubing was clamped and welded closed. All the welding steps were performed in an argon-filled glove box. Details of ARC sample preparation can be found in Ref. [27].

The ARC experiment starting temperature was usually set at 100 $^\circ\text{C}$ but was reduced to as low as 60 $^\circ\text{C}$ in some cases when exothermic reactions were detected even as low as 100 $^\circ\text{C}$. Experiments were stopped at 350 $^\circ\text{C}$ or when the self-heating rate was higher than 20 $^\circ\text{C}/\text{min}$. Exothermic reactions were tracked under adiabatic conditions when the sample self-heating rate exceeded 0.04 $^\circ\text{C}/\text{min}$. Detailed ARC sample preparation procedures and ARC operating parameters can be found in Ref. [28].

3. Results and discussion

Table 1 shows the ionic conductivity and viscosity at 20 $^\circ\text{C}$ of six of the ionic liquids used in this work. The table shows that the ionic liquids with higher conductivity have lower viscosity. With the imidazolium cation (EMI^+), the FSI^- anion shows higher conductivity than TFSI^- . On the other hand when the anion was fixed (TFSI^-) and the cation was changed, the imidazolium cation had the highest conductivity, in the following order $\text{EMI}^+ > \text{BMMI}^+ > \text{TMBA}^+ > \text{Pp13}^+$.

Fig. 2 shows the self-heating rate (SHR) versus temperature for 40 mg Li_1Si and 40 mg (a) EMI-FSI, (b) EMI-TFSI and (c) BMMI-TFSI (solid lines). The self-heating rate versus temperature of 40 mg Li_1Si and 40 mg ethylene carbonate (EC) (dashed

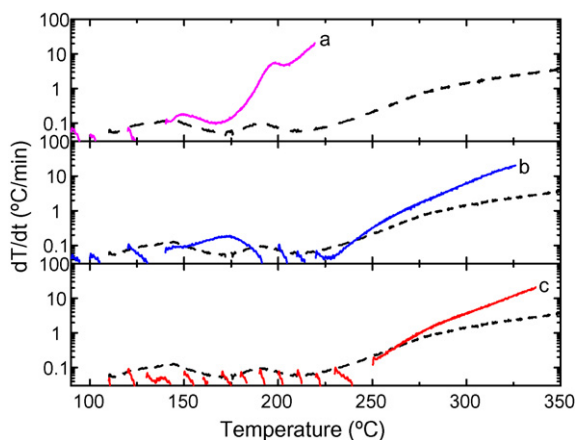


Fig. 2. Self-heating rate vs. temperature for 40 mg Li_1Si and 40 mg (a) EMI-FSI, (b) EMI-TFSI, and (c) BMMI-TFSI, respectively (solid lines). The self-heating rate vs. temperature for 40 mg Li_1Si and 40 mg EC (dashed lines) is shown in all panels for comparison.

line) is shown in all panels for comparison. Fig. 2a shows both EMI-FSI and EC have a low self-heating rate below 170 $^\circ\text{C}$. However, the self-heating rate for the EMI-FSI sample suddenly increases at about 170 $^\circ\text{C}$ and reaches 20 $^\circ\text{C}/\text{min}$ at 220 $^\circ\text{C}$ (the ARC stops the experiment once the SHR reaches 20 $^\circ\text{C}/\text{min}$). The EC sample shows a SHR less than 5 $^\circ\text{C}/\text{min}$ in the entire experimental temperature range. The self-heating rate curves in Fig. 2b and c are characterized by a relatively low reaction rate from 90 to 230 $^\circ\text{C}$ followed by an increase in reaction rate above 230 $^\circ\text{C}$. These results indicate that EMI-FSI reacts more rapidly with Li_1Si than EC, but that the reactivity of EMI-TFSI and BMMI-TFSI is similar to that of EC.

Fig. 3 compares the self-heating rate versus temperature for 40 mg Li_1Si and 40 mg (a) 1 M LiPF_6 EMI-FSI, (b) 1 M LiPF_6 EMI-TFSI, (c) 1 M LiPF_6 BMMI-TFSI (solid lines), and 1 M LiPF_6 EC:DEC (volume ratio, 1:2; dashed lines), respectively. All of the SHR curves are characterized by low SHR at low temperature followed by an increase in SHR rate at high temperature. The onset of high SHR is about 175 $^\circ\text{C}$ for LiPF_6 EMI-FSI, 250 $^\circ\text{C}$ for LiPF_6 EMI-TFSI, 270 $^\circ\text{C}$ for LiPF_6 BMMI-TFSI, and 220 $^\circ\text{C}$ for LiPF_6 EC:DEC, respectively. Figs. 2 and 3 show that in the presence of LiPF_6 , the thermal stability of the ionic liquid/ Li_1Si samples increases. The SHR curves in both Figs. 2 and 3 show low SHR at low temperature followed by increased SHR at higher temperatures. This behavior is the similar to that shown in Refs. [26,29]. At low temperature, the buildup of reaction products on the surface of the reacting particles slows further reaction. Above a certain temperature, the film of the reaction products is no longer stable and the SHR increases.

Fig. 4 shows the self-heating rate versus temperature for 150 mg $\text{Li}_7\text{Ti}_5\text{O}_{12}$ and 40 mg (a) EMI-FSI, (b) EMI-TFSI, (c) BMMI-TFSI (solid lines) and EC, respectively (dashed lines). In the top panel, the EMI-FSI/ $\text{Li}_7\text{Ti}_5\text{O}_{12}$ sample exhibits thermal runaway starting at only 70 $^\circ\text{C}$ while the EC sample exhibits runaway starting at 140 $^\circ\text{C}$, indicating that EC is safer than EMI-FSI in the presence of $\text{Li}_7\text{Ti}_5\text{O}_{12}$. The EMI-

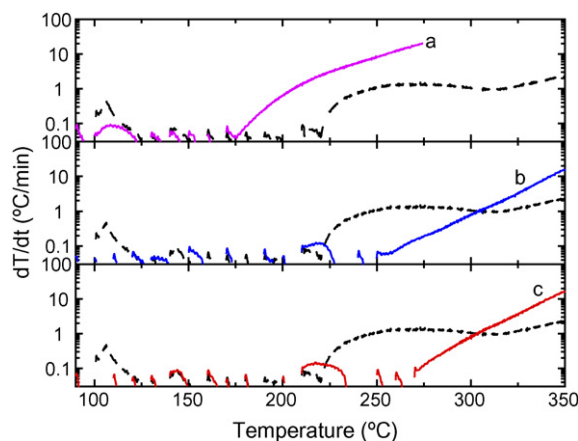


Fig. 3. Self-heating rate vs. temperature for 40 mg Li_1Si and 40 mg (a) 1 M LiPF_6 EMI-FSI, (b) 1 M LiPF_6 EMI-TFSI, and (c) 1 M LiPF_6 BMMI-TFSI, respectively (solid lines). The self-heating rate vs. temperature for 40 mg Li_1Si and 40 mg 1 M LiPF_6 EC:DEC (volume ratio: 1:2, dashed lines) is shown in all panels for comparison.

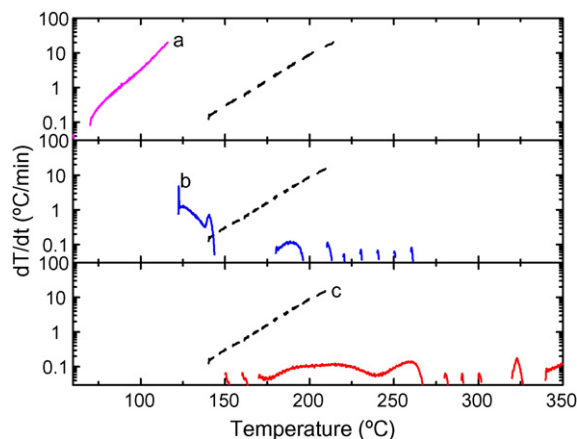


Fig. 4. Self-heating rate vs. temperature for 150 mg $\text{Li}_7\text{Ti}_5\text{O}_{12}$ and 40 mg (a) EMI-FSI, (b) EMI-TFSI and (c) BMMI-TFSI, respectively (solid lines). The self-heating rate vs. temperature for 150 mg $\text{Li}_7\text{Ti}_5\text{O}_{12}$ and 40 mg EC (dashed lines) is shown in all panels for comparison.

TFSI/ $\text{Li}_7\text{Ti}_4\text{O}_{12}$ sample (curve b) shows an initially large SHR at about 120°C , which then decreases, suggesting good passivation of the $\text{Li}_7\text{Ti}_5\text{O}_{12}$ surface by reaction products. The BMMI-TFSI/ $\text{Li}_7\text{Ti}_4\text{O}_{12}$ encounters an exothermic reaction at about 150°C but the SHR remains below about $0.1^\circ\text{C}/\text{min}$ over the entire experiment, again indicating effective passivation by reaction products.

A comparison of the reactivity of EMI-FSI, EMI-TFSI, BMMI-TFSI and EC with Li_1Si (Fig. 2) and with $\text{Li}_7\text{Ti}_4\text{O}_{12}$ (Fig. 4) is instructive. The amount of Li_1Si (40 mg) and the amount of $\text{Li}_7\text{Ti}_4\text{O}_{12}$ (150 mg) added to the ARC tubes were chosen so that the samples had the same number of moles of reactive Li atoms. However, the electrode potential of Li_1Si is near 0.2 V versus Li while that of $\text{Li}_7\text{Ti}_4\text{O}_{12}$ is near 1.55 V and the specific surface area of the samples differs greatly. The difference in the electrode potential has been shown to affect the total heat evolved in the reaction between negative electrode materials and solvents [30] and the specific surface area affects the reaction rate [1]. In all experiments in Figs. 2 and 4, the SHRs for the negative electrode materials reacting with EC ultimately reach values above $3^\circ\text{C}/\text{min}$. By contrast, even though high SHRs are reached for EMI-TFSI and BMMI-TFSI in contact with Li_1Si , high heating rates are never reached for these two solvents in contact with $\text{Li}_7\text{Ti}_4\text{O}_{12}$ in spite of its high specific surface area. Apparently EMI-TFSI and BMMI-TFSI solvents show a strong dependence of reactivity on negative electrode potential.

Fig. 5 shows the self-heating rate versus temperature for 150 mg $\text{Li}_7\text{Ti}_5\text{O}_{12}$ and 40 mg (a) 1 M LiPF_6 EMI-FSI, (b) 1 M LiPF_6 EMI-TFSI, (c) 1 M LiPF_6 BMMI-TFSI (solid lines) and 1 M LiPF_6 EC:DEC (volume ratio, 1:2; dashed lines), respectively. In the top panel the EMI-FSI/ $\text{Li}_7\text{Ti}_5\text{O}_{12}$ sample starts a strong exothermic reaction at 60°C , and proceeds to thermal runaway at about 130°C . By comparison to curve (a) in Fig. 4, it is clear that the addition of LiPF_6 has little impact on the reactivity of $\text{Li}_7\text{Ti}_5\text{O}_{12}$ and EMI-FSI. The reaction between 1 M LiPF_6 EC:DEC and $\text{Li}_7\text{Ti}_5\text{O}_{12}$ begins around 200°C in good agreement with Fig. 8b in Ref. [30]. The reaction between 1 M LiPF_6 EMI-TFSI and $\text{Li}_7\text{Ti}_5\text{O}_{12}$ described by curve (b) in Fig. 5

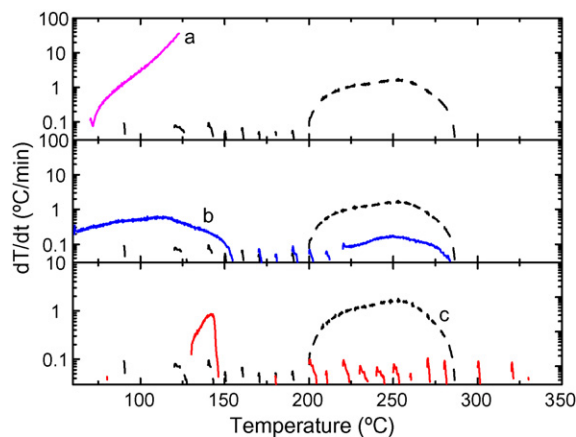


Fig. 5. Self-heating rate vs. temperature for 150 mg $\text{Li}_7\text{Ti}_5\text{O}_{12}$ and 40 mg (a) 1 M LiPF_6 EMI-FSI, (b) 1 M LiPF_6 EMI-TFSI and (c) 1 M LiPF_6 BMMI-TFSI, respectively (solid lines). The self-heating rate vs. temperature for 150 mg $\text{Li}_7\text{Ti}_5\text{O}_{12}$ and 40 mg 1 M LiPF_6 EC:DEC (volume ratio: 1:2, dashed lines) is shown in all panels for comparison.

begins at 60°C but proceeds relatively slowly. However, such a low onset temperature is cause for significant concern. The reaction between 1 M LiPF_6 BMMI-TFSI and $\text{Li}_7\text{Ti}_5\text{O}_{12}$ sample shows no obvious exothermic reaction in the entire measurement range except for a small exothermic reaction between 130 and 155°C . As in Fig. 4, these results indicate that for reactivity with $\text{Li}_7\text{Ti}_5\text{O}_{12}$, 1 M LiPF_6 EMI-FSI electrolyte is the most reactive and 1 M LiPF_6 BMMI-TFSI is the least reactive.

Fig. 6 shows the self-heating rate versus temperature for 100 mg $\text{Li}_{0.45}\text{CoO}_2$ and 100 mg (a) EMI-FSI, (b) EMI-TFSI, (c) BMMI-TFSI (solid lines) and EC (dashed lines), respectively. The EC/ $\text{Li}_{0.45}\text{CoO}_2$ sample begins to react strongly at 150°C and reaches the stop rate ($20^\circ\text{C}/\text{min}$) at 225°C . By contrast, none of the ionic liquid/ LiCoO_2 samples react appreciably below 210°C . Of the ionic liquids, only the EMI-FSI/ $\text{Li}_{0.45}\text{CoO}_2$ sample (curve (a)) eventually reaches the stop rate at 325°C . The BMMI-TFSI/ $\text{Li}_{0.45}\text{CoO}_2$ sample shows extremely low self-heating rate over the entire temperature range.

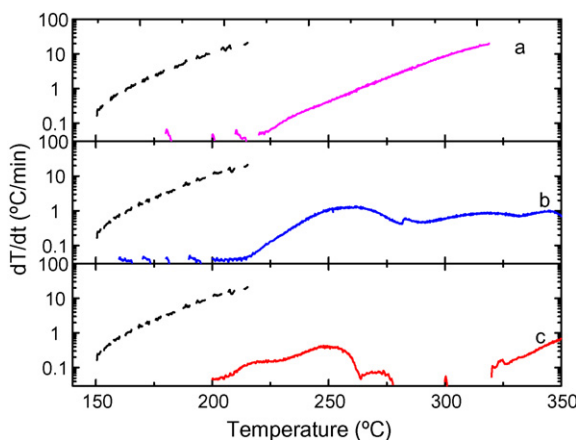


Fig. 6. Self-heating rate vs. temperature for 100 mg $\text{Li}_{0.45}\text{CoO}_2$ and 100 mg (a) EMI-FSI, (b) EMI-TFSI, and (c) BMMI-TFSI, respectively (solid lines). The self-heating rate vs. temperature for 100 mg $\text{Li}_{0.45}\text{CoO}_2$ and 100 mg EC (dashed lines) is shown in all panels for comparison.

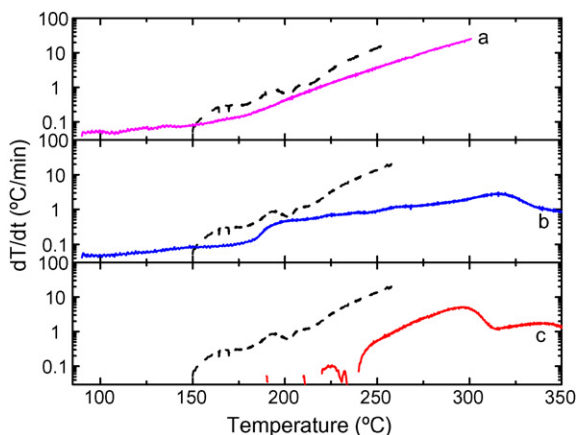


Fig. 7. Self-heating rate vs. temperature for 100 mg $\text{Li}_{0.45}\text{CoO}_2$ and 100 mg (a) 1 M LiPF_6 EMI-FSI, (b) 1 M LiPF_6 EMI-TFSI and (c) 1 M LiPF_6 BMMI-TFSI, respectively (solid lines). The self-heating rate vs. temperature for 100 mg $\text{Li}_{0.45}\text{CoO}_2$ and 100 mg 1 M LiPF_6 EC:DEC (volume ratio: 1:2; dashed line) is shown in all panels for comparison.

Fig. 7 compares the self-heating rate versus temperature for 100 mg $\text{Li}_{0.45}\text{CoO}_2$ and 100 mg (a) 1 M LiPF_6 EMI-FSI, (b) 1 M LiPF_6 EMI-TFSI, (c) 1 M LiPF_6 BMMI-TFSI (solid lines) and 1 M LiPF_6 EC:DEC (volume ratio, 1:2; dashed lines), respectively. The SHR curves for 1 M LiPF_6 EMI-FSI/ $\text{Li}_{0.45}\text{CoO}_2$ and 1 M LiPF_6 EMI-TFSI/ $\text{Li}_{0.45}\text{CoO}_2$ show similar characteristics, a low SHR beginning at 90 °C and increasing steadily up to 300 °C. Both ionic liquid samples are less reactive than the corresponding sample based on EC. A comparison of curves (a) and (b) in Figs. 6 and 7 suggest the low-self-heating rate region below 180 °C in Fig. 7 is caused by the addition of LiPF_6 . By contrast to the EMI-FSI/ $\text{Li}_{0.45}\text{CoO}_2$ and EMI-TFSI/ $\text{Li}_{0.45}\text{CoO}_2$ samples, curves (c) in Figs. 6 and 7 show the addition of LiPF_6 to BMMI-TFSI/ $\text{Li}_{0.45}\text{CoO}_2$ does not change the reaction behavior below 200 °C, but some exothermic reaction begins at about 220 °C. Nevertheless, the onset temperature for reactions of 1 M LiPF_6 BMMI-TFSI with $\text{Li}_{0.45}\text{CoO}_2$ (220 °C) is 70 °C higher than that of the 1 M LiPF_6 EC:DEC/ $\text{Li}_{0.45}\text{CoO}_2$ sample (150 °C).

The ionic liquids show a strong dependence of reactivity on the type of electrode material tested. The ionic liquids we tested show increased thermal stability compared with traditional organic solvents when $\text{Li}_{0.45}\text{CoO}_2$ is used. However, the safety properties are varied when anode materials are tested. In general, the reactivity of EMI-TFSI with both charged positive and negative electrode materials is less than that of EMI-FSI as shown in Figs. 2–7, so the TFSI[−] anion is thought to be “better” than FSI[−]. Correspondingly, the BMMI⁺ cation is “better” than EMI⁺, because BMMI-TFSI shows higher thermal stability than EMI-TFSI in all the tests described by Figs. 2–7. Fig. 1 shows that the TFSI[−] anion contains more F atoms than FSI[−]. At Li-containing negative electrodes, these F atoms may react to form LiF, which is an effective component of the passivation film. We speculate that ionic liquid molecules with a higher fluorine content can form a thicker and more stable film of reaction products, which leads to better thermal stability for TFSI[−] compared to FSI[−].

In order to investigate the impact of different anions and cations on the reactivity of ionic liquids with charged posi-

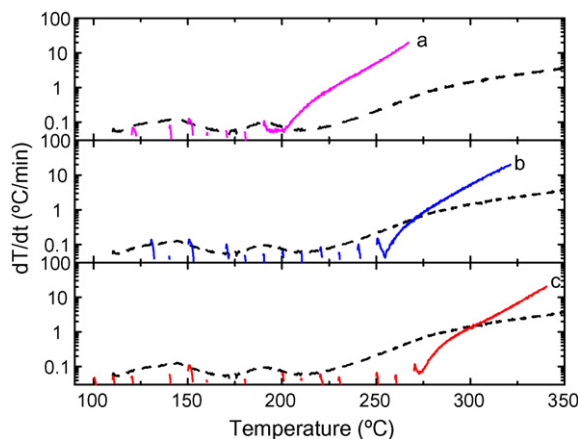


Fig. 8. Self-heating rate vs. temperature for 40 mg Li_1Si and 40 mg (a) Py13-FSI, (b) Pp14-TFSI, and (c) TMBA-TFSI, respectively (solid lines). The self-heating rate vs. temperature for 40 mg Li_1Si and 40 mg EC (dashed lines) is shown in all panels for comparison.

tive and negative electrode materials, another three ionic liquids were studied. Fig. 8 shows the self-heating rate versus temperature for 40 mg Li_1Si and 40 mg (a) Py13-FSI, (b) Pp14-TFSI, (c) TMBA-TFSI (solid lines) and EC (dashed lines), respectively. The SHR curves of Py13-FSI/ Li_1Si , Pp14-TFSI/ Li_1Si and TMBA-TFSI/ Li_1Si are characterized by very low SHR until the onset of thermal runaway at 200 °C, 255 °C and 275 °C, respectively. The EC/ Li_1Si sample begins an obvious increase in self-heating rate at 220 °C. Compared with the curves in Fig. 2, Py13-FSI/ Li_1Si is less reactive than EMI-FSI/ Li_1Si , but Pp14-TFSI/ Li_1Si and TMBA-TFSI/ Li_1Si show similar reactivity to BMMI-TFSI/ Li_1Si .

Fig. 9 shows the self-heating rate versus temperature for 150 mg $\text{Li}_7\text{Ti}_5\text{O}_{12}$ and 40 mg (a) Py13-FSI, (b) Pp14-TFSI, (c) TMBA-TFSI (solid lines) and EC (dashed lines), respectively. In the top panel, the Py13-FSI/ $\text{Li}_7\text{Ti}_5\text{O}_{12}$ sample shows negligible self-heating until 125 °C when a sustained exotherm begins, similarly to the EC/ $\text{Li}_7\text{Ti}_5\text{O}_{12}$ sample. In the middle and the bottom panels of Fig. 9, the Pp14-TFSI/ $\text{Li}_7\text{Ti}_5\text{O}_{12}$

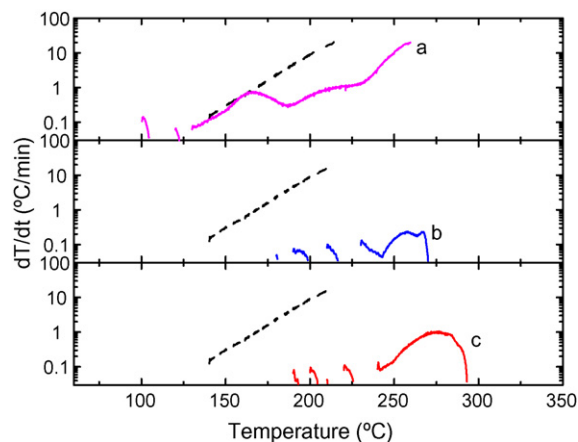


Fig. 9. Self-heating rate vs. temperature for 150 mg $\text{Li}_7\text{Ti}_5\text{O}_{12}$ and 40 mg (a) Py13-FSI, (b) Pp14-TFSI and (c) TMBA-TFSI, respectively (solid lines). The self-heating rate vs. temperature for 150 mg $\text{Li}_7\text{Ti}_5\text{O}_{12}$ and 40 mg EC (dashed lines) is shown in all panels for comparison.

and TMBA-TFSI/Li₇Ti₅O₁₂ samples show similar reaction behaviors, characterized by a discontinuous low SHR beginning at about 180 °C, with no visible exothermic reaction after 290 °C. Comparing to Fig. 4, the reactivity of Py13-FSI/Li₇Ti₅O₁₂ is similar to EC/Li₇Ti₅O₁₂ and is less than EMI-FSI/Li₇Ti₅O₁₂. The reactivity of Pp14-TFSI/Li₇Ti₅O₁₂ and TMBA-TFSI/Li₇Ti₅O₁₂ is much weaker than EC/Li₇Ti₅O₁₂ and similar to BMMI-TFSI/Li₇Ti₅O₁₂.

4. Conclusions

Using accelerating rate calorimetry (ARC), the reactivity between six ionic liquids (with and without added LiPF₆) and charged electrode materials is compared to the reactivity of standard carbonate-based solvents and electrolytes with the same electrode materials. The charged electrode materials used were Li₁Si, Li₇Ti₄O₁₂ and Li_{0.45}CoO₂. The experiments showed that not all ionic liquids are safer than commonly used electrolytes/solvents (EC, 1 M LiPF₆ EC DEC). Of the six ionic liquids tested, EMI-FSI shows the worst safety properties, and is much worse than conventional electrolyte. EMI-TFSI and Py13-FSI show similar reactivity to carbonate-based electrolyte. The three ionic liquids BMMI-TFSI, Pp14-TFSI and TMBA-TFSI show similar reactivity and are much safer than the conventional carbonate based electrolyte. A comparison of the reactivity of ionic liquids with common anions and cations showed that ionic liquids with TFSI⁻ are safer than those with FSI⁻, and liquids with EMI⁺ are worse than those with BMMI⁺, Py13⁺, Pp14⁺ and TMBA⁺.

Acknowledgements

YW and JRD acknowledge funding from 3M Canada Co. and NSERC. FFCB and RMT acknowledge FAPESP (Proc. 03/10015-3), CNPq and CAPES (Brazilian funding agencies) for financial support.

References

- [1] D.D. MacNeil, D. Larcher, J.R. Dahn, *J. Electrochem. Soc.* 146 (1999) 3596.

- [2] D.D. MacNeil, Z.H. Lu, Z.H. Chen, J.R. Dahn, *J. Power Sources* 108 (2002) 8.
- [3] J. Jiang, J.R. Dahn, *Electrochim. Acta* 49 (2004) 4599.
- [4] Y.S. Fung, R.Q. Zhou, *J. Power Sources* 81/82 (1999) 891.
- [5] B. Garcia, S. Lavallee, G. Perron, C. Michot, M. Armand, *Electrochim. Acta* 49 (2004) 4583.
- [6] Y. Abu-Lebdeh, A. Abouimrane, P.-J. Alarco, M. Armand, *J. Power Sources* 154 (2006) 255.
- [7] H. Sakaebe, H. Matsumoto, *Electrochem. Commun.* 5 (2003) 594.
- [8] H. Nakagawa, S. Izuchi, K. Kuwana, T. Nukuda, Y. Aihara, *J. Electrochem. Soc.* 150 (2003) 594.
- [9] E. Markevich, V. Baranchugov, D. Aurbach, *Electrochem. Commun.* 8 (2003) 1331.
- [10] S. Seki, Y. Kobayashi, H. Miyashiro, Y. Ohno, A. Usami, Y. Mita, M. Watanabe, N. Terada, *Chem. Commun.* (2006) 544.
- [11] S. Seki, Y. Kobayashi, H. Miyashiro, Y. Ohno, A. Usami, Y. Mita, N. Kihira, M. Watanabe, N. Terada, *J. Phys. Chem. B* 110 (2006) 10228.
- [12] M. Ishikawa, T. Sugimoto, M. Kikuta, E. Ishiko, M. Kono, *J. Power Sources* 162 (2006) 658.
- [13] H. Matsumoto, H. Sakaebe, K. Tatsumi, M. Kikuta, E. Ishiko, M. Kono, *J. Power Sources* 160 (2006) 1308.
- [14] H. Sakaebe, H. Matsumoto, K. Tasumi, *Electrochim. Acta*, 2007, doi:10.1016/j.electacta.2007.02.054.
- [15] M. Galinski, A. Lewandowski, I. Stepniak, *Electrochim. Acta* 51 (2006) 5567.
- [16] F. Endres, S.Z.E. Abedin, *Phys. Chem. Chem. Phys.* 8 (2006) 2101.
- [17] M. Egashira, M. Tanaka-Nakagawa, I. Watanabe, S. Okada, J.-I. Yamaki, *J. Power Sources* 160 (2006) 1387.
- [18] K. Zaghbi, D. Brouillette, M. Armand, Hydro Quebec Internal report, July 1999.
- [19] M. Armand et al., US Patent 6,365,301 (2002).
- [20] K. Zaghbi, J. Jalbert, A. Guerfi, Canadian patent application, submitted for publication.
- [21] M. Morita, Y. Asai, N. Yoshimoto, M. Ishikawa, *J. Chem. Soc., Faraday Trans.* 94 (1998) 3451.
- [22] A.K. Srivastava, R.A. Samant, S.D. Patankar, *J. Chem. Eng. Data* 41 (1996) 431.
- [23] D.Y.W. Yu, K. Donoue, T. Inoue, M. Fujimoto, S. Fujitani, *J. Electrochem. Soc.* 153 (2006) A835.
- [24] F.F.C. Bazito, L.T. Silveira, R.M. Torresi, S.I. Córdoba de Torresi, *Electrochim. Acta* (2007), doi:10.1016/j.electacta.2006.12.055.
- [25] D.D. MacNeil, Ph.D. Thesis, Dalhousie University, 2001.
- [26] Y. Wang, J. Dahn, *Electrochem. Solid State Lett.* 9 (2006) A340.
- [27] D.D. MacNeil, S. Trussler, H. Fortier, J.R. Dahn, *Thermochim. Acta* 386 (2002) 153.
- [28] M.N. Richard, J.R. Dahn, *J. Electrochem. Soc.* 146 (1999) 2068.
- [29] M.N. Richard, J.R. Dahn, *J. Electrochem. Soc.* 146 (1999) 2078.
- [30] J. Jiang, J.R. Dahn, *J. Electrochem. Soc.* 153 (2006) A310.